Prevention of steel reinforcement corrosion in alkali-activated slag cement concrete mixed with seawater

Pavlo Krivenko[1], *Igor* Rudenko[1], *Oleksandr* Konstantynovskyi[1,*], and *Olha* Boiko[1]

[1]Kyiv National University of Construction and Architecture, Scientific Research Institute for Binders and Materials, 31 Povitroflotskyi Ave., Kyiv, 03037, Ukraine

Abstract. Concretes mixed with seawater are characterised by enhanced performances, but action of chlorides and sulfates ensures the risk of reinforcement corrosion. Application of high consistency fresh concretes ensures changes in hardened concrete structure that causes the problem of steel reinforcement passive state ensuring. Thus mixing of plasticized concretes by seawater actualizes the search for means of steel corrosion prevention. Alkali-activated slag cements (further, AASC's) reduce effect of ions Cl^- and SO_4^{2-} on steel reinforcement in concrete due to their exchange for ions OH^- in the structure of zeolite-like alkaline hydroaluminosilicates. Complex additive «portland cement - calcium aluminate cement - clinoptilolite» was proposed to enhance the protective properties of AASC concretes to steel reinforcement. The results of DTA, X-ray diffraction, electron microscopy, microprobe analysis show that complex additive ensures to prevent steel reinforcement corrosion in AASC concrete mixed with seawater due to binding Cl^- and SO_4^{2-} ions in Kuzel's salt in AASC hydration products and exchange of these aggressive ions with OH^- ions in the structure of clinoptilolite. This effect of complex additive confirmed by surface state and the absence of mass loss of steel rebars embedded in plasticized AASC fine concrete mixed with seawater after 90 d of hardening.

1 Introduction

The actuality of green materials implementation is due to their conformity with modern tendencies in construction engineering concerning efficient consumption of raw materials and energy resources [1], as well as responsible attitude to ecology of the environment [2]. Cements, which contain inorganic additives, fully comply modern tendencies for sustainable development of mankind [3]. The ecological benefits of such cements are caused by reduction of CO_2 emission due to substitution of portland cement clinker by inorganic additives [4]. At that, materials based on the mentioned cements are characterized by high quality, functionality and durability. Efficiency of high early strength multicomponent cements based on ground blast furnace slags (further, GBFS), zeolite and fly-ash in mortars was shown [5]. Additives of polydisperse zeolite tuff and perlite provide positive effect on concrete strength in different conditions [6]. Addition of zeolite or highly dispersed chalk enhances strength of cements [7], as well as crack resistance [8] and freeze-thaw resistance of concretes [9]. Portland cements containing GBFS are characterized by increased corrosion resistance and can be used in protective materials [10].

Alkali-activated slag cement (further, AASC) can be consider as the most perspective environmentally friendly ones. Alkali activation of aluminosilicate raw materials is widely used [11, 12]. The ecological benefits of AASC's are caused by reduction of CO_2 emission while consumption of by-products as well as waste products [13]. AASC mortars and concretes are characterized by increased strength [14], heat resistance [15, 16], corrosion resistance [17], freeze-thaw resistance [18], waterproof [19] and fire resistance [20, 21] in comparison with analogues based on traditional clinker cements. Beside of high performances, AASC's can be used in decorative materials [22]. Radioactive wastes [23] and manufacturing waters [24] are effectively used in safety building materials based on AASC.

As perspective direction being taken to improve the environmental friendliness of modern concretes, has been using of seawater. It's known, that the consumption of water in concrete is 9 % of the total consumption of industrial water [25]. Thus, the most recent substantial interest has been placed on seawater as an alternative solution for impeding the exploitation of freshwater.

Seawater can be used as an activator of GBFS's hydraulic properties [26, 27, 28]. This phenomena is caused by salts of strong acids (further, SSA's), like chlorides and sulfates, dissolved in seawater [29, 30]. At that, seawater ensures increasing of AASC concrete consistency [31] and concrete strength [32] that is explained by effect of SSA's [33, 34].

However, corrosion of steel reinforcement under action of chlorides and sulfates is the main problem for concretes mixed with seawater. There are two main processes during corrosion action on steel reinforcement: carbonation and pitting corrosion, caused by chlorine-ions [35]. Sulfate-ions don't cause immediate depassivation of steel reinforcement, but determine formation of hydrogen

* Corresponding author: alexandrkp@gmail.com

sulfide (H_2S), which catalyze oxidation (carbonation) of hydrate phases.

The stability of passive film on the surface of steel reinforcement in AASC concrete, mixed with seawater, depends on concentration of free chlorine-ions and OH^- ions in pore solution, primarily in contact zone between reinforcement and concrete [36]. The passive state of steel reinforcement is provided at molar ratio of $Cl^-/OH^- \leq 0.6$ in pore solution [37].

The modern requirements to high consistency fresh concretes are governed by practice. This way the disturbance of reinforcement passive state can be caused by changes in hardened concrete structure [38]. Problem with ensuring of steel reinforcement passive state in AASC concretes, mixed with seawater, is intensified. Thus, the means for protection of steel reinforcement in plasticized AASC concretes must be developed.

It was shown, that the modification by complex additive (further, CAD) based on SSA's ensures decreasing of AASC concrete drying shrinkage as well as enhancement of crack resistance [39]. This type of modification provides mitigation of steel reinforcement corrosion. Effect of CAD is caused by less water, acceleration of crystallization, alteration of porous structure as well as by changes in morphology of hydrated phases [33, 34].

One of the ways to prevent the steel reinforcement corrosion in AASC concrete mixed with seawater is decreasing of chlorine ions in pore solution due to their binding in low soluble compounds. It's well-known that hydration products of AASC are able to bind chlorine-ions. Alkaline hydroaluminosilicates, as analogues of natural zeolites, can be refered as such phases [29]. Apart from alkaline hydroaluminosilicates, free chlorine can be binded in Cl-bearing phases like hydrotalcite $[Mg_3Al(OH)_8]Cl \cdot 3H_2O$ and hydrocalumite $3CaO \cdot Al_2O_3 \cdot CaCl_2 \cdot 10H_2O$ [40]. These phases are suitable for chlorine binding both due to exchange processes and physical adsorption [41, 42, 43]. It was shown the binding of chlorine-ions by hydrosilicate C–S–H and hydroaluminosilicate C–A–S–H gel phases [44, 45].

Formation of phases, which provide binding of Cl^- and SO_4^{2-} ions, was proposed to prevent steel reinforcement corrosion in AASC concrete. It's well-known that chlorine can be binded by tricalcium aluminate ($3CaO \cdot Al_2O_3$) in AFm phases (Al_2O_3-Fe_2O_3-mono), which are characterized by greater stability comparing to AFt phases (ettringite) while increasing alkalinity of hydration medium [46, 47, 48]. The AFm phases can include different anions (Cl^-, SO_4^{2-}, CO_3^{2-}, OH^- etc.). Thus, AFm phases can be presented by monocarboaluminate, hemicarboaluminate, stratlingite, hydroxyl-AFm and monosulfoaluminate [49]. It was shown formation of nitrate containing AFm phase along with chloride and sulfate containing ones [50].

The above results cause reasonable application of calcium aluminate cement and portland cement as additives in AASC to ensure formation of highly-calcium hydroaluminates $3CaO \cdot Al_2O_3 \cdot 10H_2O$ for prevention of steel reinforcement corrosion due to binding of Cl^- and SO_4^{2-} ions. Highly-calcium hydroaluminates $3CaO \cdot Al_2O_3 \cdot 10H_2O$ can be formed due to interaction of portlandite $Ca(OH)_2$ (hydration product of portland cement) with low-calcium hydrosilicates (hydration product of calcium aluminate cement) [51]:

$$CaO \cdot Al_2O_3 \cdot (6 \ldots 8)H_2O + 2Ca(OH)_2 \rightarrow$$
$$\rightarrow 3CaO \cdot Al_2O_3 \cdot 10H_2O \quad (1)$$

$3CaO \cdot Al_2O_3 \cdot 10H_2O$ ensures binding Cl^- and SO_4^{2-} ions in low soluble AFm phases [52]:

$$3CaO \cdot Al_2O_3 \cdot 10H_2O + Cl^-, SO_4^{2-} + H_2O \rightarrow$$
$$\rightarrow 3CaO \cdot Al_2O_3 \cdot CaCl_2(SO_4) \cdot 10H_2O \quad (2)$$

Application of aluminosilicate ionites such as clinoptilolite (natural zeolite) in AASC concrete composition, mixed with seawater, can be mean for prevention of steel reinforcement corrosion. Zeolites are known, first of all, as cationites which exchange Na^+ ions with Ca^{2+} ions, but can also act like anionites to exchange OH^- ions with Cl^- and SO_4^{2-} ions [53]. Clinoptilolite supplements anionite function of alkaline hydroaluminosilicates (analogues of natural zeolites) during AASC hydration.

The above results allow predicting prevention of steel reinforcement corrosion in plasticized AASC concrete mixed with seawater due to application of CAD «portland cement - calcium aluminate cement - clinoptilolite».

The aim of this research was to investigate the effect of seawater on the performances of plasticized AASC concrete and to ensure prevention of steel reinforcement corrosion due to application of CAD «portland cement - calcium aluminate cement - clinoptilolite».

2 Raw materials and methods

GBFS (CaO – 47.30 %; SiO2 – 39.00 %; Al_2O_3 – 5.90 %; Fe_2O_3 – 0.30 %; MgO – 5.82 %; SO_3 – 1.50 %; TiO_2 – 0.31 %), basicity modulus= 1.11, content of glass phase= 84.0 %, specific surface= 450 m^2/kg (by Blaine), was used as an aluminosilicate component of AASC.

Alkaline components of AASC were presented by:

- soda ash (Na_2CO_3), dry state;
- five-water sodium metasilicate ($Na_2SiO_3 \cdot 5H_2O$), dry state;

Two reference compositions of AASC were used:

- based on soda ash (GBFS – 93.50 %, soda ash – 6.50 % (3.80 % by Na_2O));
- based on sodium metasilicate (GBFS – 88.50 %, sodium metasilicate – 11.50 % (3.36 % by Na_2O));

The AASC's were also modified by CAD, which components were presented by:

- portland cement CEM I 42,5 R (PJSC Ivano-Frankivskcement, Ukraine);
- calcium aluminate cement ISTRA 40 (HeidelbergCement, Germany);
- natural zeolite (clinoptilolite) powder (by mass, %: SiO_2 – 72.5, Al_2O_3 – 13.1, Fe_2O_3 – 0.9, TiO_2 – 0.2, CaO – 2.1, MgO – 1.07, P_2O_5 – 0.003, K_2O+Na_2O – 5.03), fr. 0 - 0.1 mm, content of clinoptilolite ≤ 93.0 %, porosity 54.0 % (JSC Zeolite-Bio, Ukraine).

Content of CAD was 10.00 % by mass of AASC. Contents of CAD components, %: (portland cement + calcium aluminate cement) – 5, clinoptilolite – 5.

The ratio between portland cement and calcium aluminate cement was 2.17:1.00 taking into account formation of $3CaO{\cdot}Al_2O_3{\cdot}10H_2O$ according to reaction (1).

Surfactants were presented by:

- sodium lignosulphonate (further, LST) according to CAS 8061-51-6 (pH ≥ 8.5);
- sodium gluconate according to CAS 527-07-1.

AASC's were mixed with fresh water or with seawater, which was presented by aqueous solution of salts, % by mass of mixture: NaCl – 78.70, $MgCl_2$ – 9.80, $MgSO_4$ – 5.76, $CaSO_4$ – 3.75, KCl – 1.73, $CaCO_3$ – 0.29. Total concentration of seawater salts was 35 g/l.

The standard quartz sand according to EN 196-1 was used in AASC fine aggregate concretes (ratio AASC to sand = 1:3).

Reinforcement was presented by steel rebars, length 120 mm and diameter 4.1 - 4.3 mm.

Fresh concretes were prepared in mixer «Raimondi Iperbet» (Italy).

Consistency (workability) was determined by cone slump according to the national standard of Ukraine DSTU B V.2.7-114:2002.

Consistency class of fresh concrete was S4 (slump 160 - 210 mm).

The performances plasticized of AASC concretes (AASC:sand = 1:3) were determined on specimens 40x40x160 mm.

The state of embedded steel rebars in plasticized AASC concrete, mixed with seawater, was estimated according to following method. The basic rebars, length (120±2) mm and diameter from 3 to 6 mm, were embedded in specimens 40x40x160 mm of AASC concrete. These rebars were degreased by acetone and weighted with accuracy of ±0,001 g before embedding. After hardening of specimens in normal conditions (*t*=20±2 °C, *R.H.*=95±5 %) the basic rebars were reached from AASC concrete and etched during (25±5) min in 10 % solution of hydrochloric acid with adding of urotropine (1 % by acid mass) to remove rests of cement stone and products of corrosion. The reference rebars, which weren't embedded in concrete, were weighted and etched simultaneously with basic rebars. After etching the basic and reference rebars were cleaned by distilled water and were immersed in fat solution of sodium nitrate for 5 min. Then the rebars were wiped by filter paper, dried up and weighted. The mass loss of rebars were calculated as a ratio of mean differences between masses before and after etching to surface area.

Monitoring the structure formation was carried out by X-ray diffraction (XRD), differential-thermal analysis (DTA) and electronic microscope with microanalyzer

3 Results and discussion

Effect of CAD «portland cement - calcium aluminate cement - clinoptilolite» on structure formation of AASC, mixed with seawater, was investigated.

3.1 Structure formation of alkali-activated slag cement based on soda ash and mixed with seawater

XRD indicates the slightly crystallized low-calcium hydrosilicates such as CSH(B) (d= 0.307; 0.280; 0.183 nm) and gyrolite $2CaO{\cdot}3SiO_2{\cdot}2H_2O$ (d= 0.33; 0.268; 0.180 nm) after 90 d of hydration (Fig.1, curve 1). Besides, calcite (d= 0.307; 0.191; 0.160; 0.152 nm) is formed. Specified phases are typical for AASC [54].

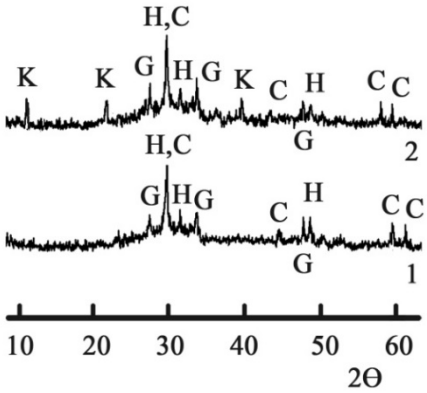

Fig. 1. XRD of alkali-activated slag cement mixed with seawater and hydrated during 90 d: 1 – the reference; 2 - modified by complex additive. Legend: H – calcium hydrosilicates CSH(B), G – gyrolite, C – calcite, K – Kuzel`s salt.

Clorine- and sulfate-binding zeolite-like minerals, which are similar to nosean $Na_8(Al_6Si_6O_{24})(SO_4){\cdot}H_2O$, sodalite $Na_4(Si_3Al_3)O_{12}Cl$, cancrinite $(Na,Ca)_8(Al_6Si_6O_{24})(CO_3,SO_4)_2{\cdot}2H_2O$ etc., can be predicted [29, 55]. However these hydrates were not identified because of their submicrocristalline state.

DTA confirms formation of slightly crystallized calcium hydrosilicates CSH(B) by endothermic effect at t= 175 (dehydration) and exothermic effect at t= 865 °C (recrystallization into wollastonite). The endothermic effects at t= 175 and 700 °C (stepped dehydration) and exothermic effect at t= 865 °C (recrystallization into wollastonite) are typical for gyrolite $2CaO{\cdot}3SiO_2{\cdot}2H_2O$ (Fig. 2, curve 1). The endothermic effect at t= 890 °C confirms presence of $CaCO_3$ (Fig. 2, curve 1).

According to electron microscopy (Fig.3 a), gel-like low-calcium hydrosilicates CSH(B) (content in probe, %: CaO – 30.19, SiO_2 - 35.42) (Fig.3 b) and prismatic formations of calcite $CaCO_3$ (content in probe, %: CaO - 53.78, CO_2 - 41.29) (Fig.3 c) were identified in the reference AASC.

Chlorine and sulfate containing AFm phases, known as Kuzel's salt $3CaO{\cdot}Al_2O_3{\cdot}0{,}5CaCl_2{\cdot}0{,}5SO_4{\cdot}10H_2O$ (d= 0.83; 0.42; 0.23 nm) [56], were also identified in hydration products of AASC, modified by CAD and mixed with seawater (Fig.1, curve 2). Specified phases were formed due to binding Cl^- and SO_4^{2-} ions by calcium hydroaluminate $3CaO{\cdot}Al_2O_3{\cdot}10H_2O$ according to reaction (2).

The presence of Kuzel's salt in hydration products of AASC, modified by CAD and mixed with seawater, was confirmed by endothermic effects at t= 330 °C (dehydration) and 480 °C (departure of chloride) as well

as by exothermic effect at t= 1000 °C (decomposition of sulfate) (Fig. 2, curve 2). Relocation of effects to higher temperatures ensures formation of CSH(B) and gyrolite with advanced crystallization.

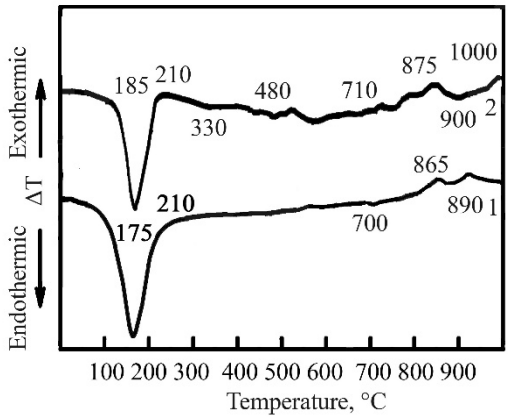

Fig. 2. DTA of alkali-activated slag cement mixed with seawater and hydrated during 90 d: 1 – the reference; 2 - modified by complex additive.

a)

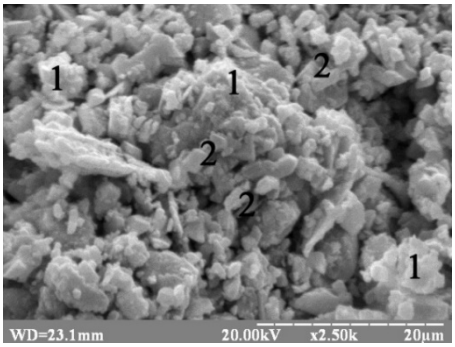

b)

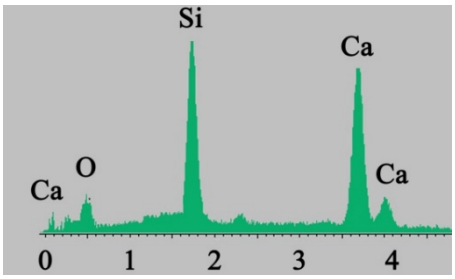

c)

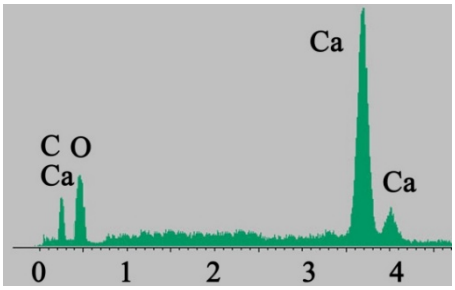

Fig. 3. Microstructure of the reference alkali-activated slag cement mixed with seawater and hydrated during 90 d: a – SEM images; b, c – microprobe analysis in points 1, 2 agreeably.

a)

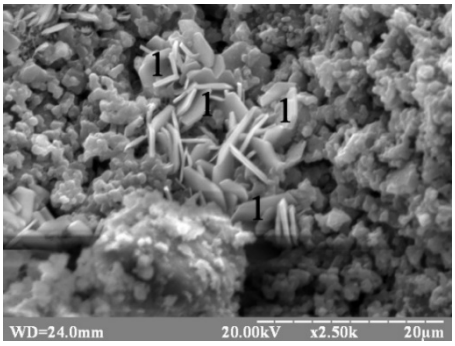

b)

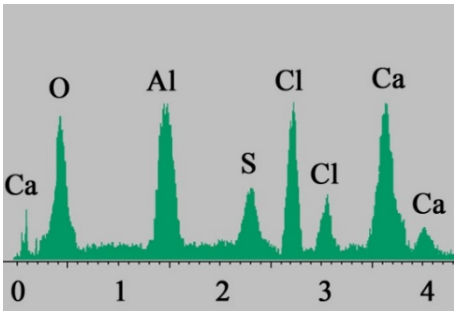

Fig. 4. Microstructure of the reference alkali-activated slag cement mixed with seawater and hydrated during 90 d: a – SEM images; b – microprobe analysis in points 1.

The modification of AASC by CAD causes formation of low-calcium hydrosilicates with a higher level of crystallization as well as hexagonal thin plates of Kuzel's salt (Fig. 4 a). The content of oxides confirms formation of Kuzel's salt, %: CaO – 32,72, Al_2O_3 – 21,51, Cl – 10,27, SO_3 – 9,56) (Fig.4 b).

3.2 Structure formation of alkali-activated slag cement based on sodium metasilicate and mixed with seawater

XRD ensures formation of slightly crystallized low-calcium hydrosilicates such as CSH(B) and gyrolite (Fig.5, curve 1). The presence of zeolite-like minerals (similar to nosean, sodalite, concrinite etc. by composition), which can bind Cl^- and SO_4^{2-} ions, can be assumed.

The presence of mentioned hydrosilicates was confirmed (Fig. 6, curve 1). Gel-like low-calcium hydrosilicates CSH(B) (Fig.7 a) (content in probe, %: CaO – 32.35 SiO_2 – 34.71) can be identified in the reference AASC after 90 d of hydration (Fig.7 b).

According to XRD, low-calcium hydrosilicates and Kuzel's salt were fixed as hydration products of AASC modified by CAD (Fig.5, curve 2).

These hydrates can be confirmed by DTA (Fig. 6, curve 2). Displacement of mentioned effects to higher temperatures ensures formation of CSH(B) and gyrolite with advanced crystallization.

The phase composition of modified AASC (Fig.8 a) is represented by low-calcium hydrosilicates as well as by hexagonal thin plates of Kuzel's salt (content in probe, %:

CaO – 31.22, Al_2O_3 – 24.87, Cl – 12.43, SO_3 – 10.94) (Fig.8 b).

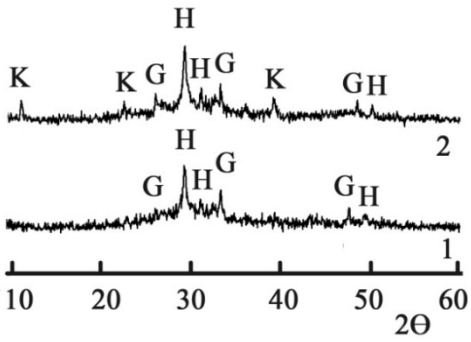

Fig. 5. XRD of 90 d hydrated alkali-activated slag cement mixed with seawater: 1 – the reference; 2 - modified by complex additive. Legend: H – calcium hydrosilicates CSH(B), G – gyrolite, K – Kuzel`s salt.

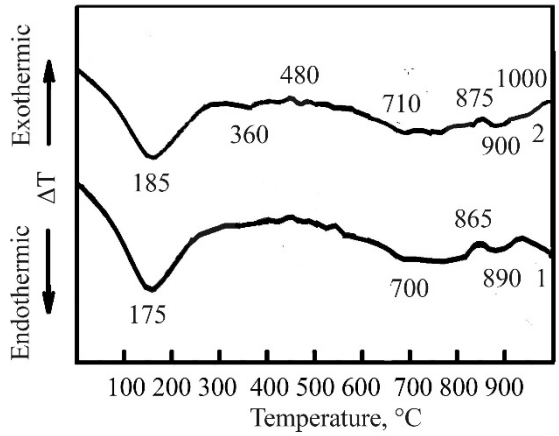

Fig. 6. DTA results of 90 d hydrated alkali-activated slag cement mixed with seawater: 1 - the reference; 2 - modified by complex additive.

Hence, CAD «portland cement - calcium aluminate cement - clinoptilolite» ensures binding of Cl- and SO_4^{2-} ions in structure of hydrated AASC based on soda ash or sodium metasilicate while mixing by seawater. Interaction between hydration products of portland cement and calcium aluminate cement provides formation of high-calcium hydroaluminates like $3CaO{\cdot}Al_2O_3{\cdot}10H_2O$, which bind the mentioned ions in Kuzel's salt. Clinoptilolite, as component of CAD, supplements action of alkaline hydroaluminosilicates (typical hydration products of AASC) with replacement of OH- ions to Cl- and SO_4^{2-} ions.

Specified structure formation of AASC, mixed with seawater, ensures prevention of steel reinforcement corrosion due to minimization of free Cl^- and SO_4^{2-} ions in pore solution of artificial stone.

3.3 Effectiveness of complex additive in alkali-activated slag cement plasticized fine concrete

The effect of CAD «portland cement - calcium aluminate cement - clinoptilolite» on protective properties of plasticized AASC fine concrete, mixed with seawater, to steel reinforcement was investigated. Mass loss of steel rebars, which were reached from plasticized AASC concrete after 90 d of hardening was fixed.

a)

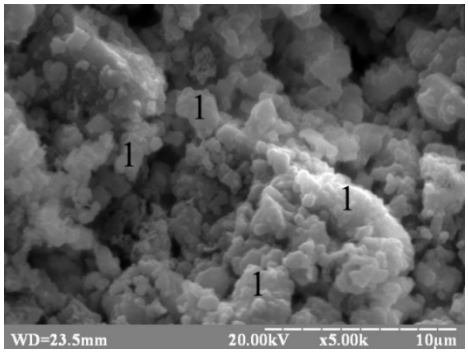

b)

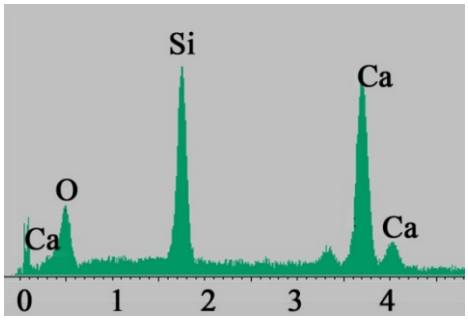

Fig. 7. Microstructure of the reference alkali-activated slag cement mixed with seawater and hydrated during 90 d: a – SEM images; b – microprobe analysis in points 1.

a)

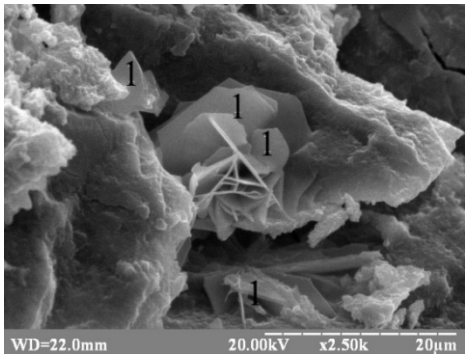

b)

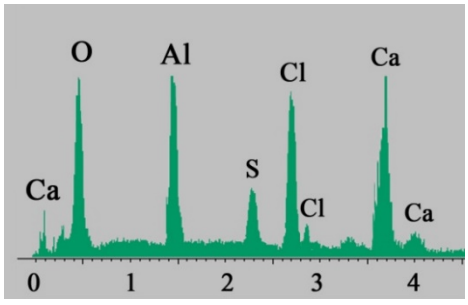

Fig. 8. Microstructure of 90 d hydrated alkali-activated slag cement, modified by CAD and mixed with seawater: a – SEM images; b – microprobe analysis in points 1.

AASC's, based on soda ash as well as on sodium metasilicate, were used as bases of fine concrete. AASC fine concrete was modificated by CAD «portland cement - calcium aluminate cement - clinoptilolite». The CAD composition, %: portland cement – 34.2, calcium aluminate cement – 15.8, clinoptilolite – 50.0. AASC fine concrete was plasticized by LST and sodium gluconate.

W/C ratios in AASC concrete based on soda ash and sodium metasilicate were 0.46 and 0.43 agreeably. W/C ratios in AASC concrete while mixing with seawater were 0.44 and 0.41 agreeably. This is evidence of AASC fresh concrete workability increasing while mixing with seawater [54]. At that, increasing of AASC concrete strength while mixing with seawater was fixed. Thus, compressive strength of AASC concrete based on soda ash while mixing with seawater corresponds to values of 35.7 MPa that is on 21.8 % greater comparing with one mixed with water (29.3 MPa). Compressive strength of AASC concrete, based on sodium metasilicate and mixed with seawater, is on 10.9 % greater comparing with one mixed with water (45.8 and 41.3 MPa agreeably). Enhancement of AASC fine concrete strength while mixing with seawater comparing with one mixed with water is caused by effect of SSA's [30, 33, 34].

The effect of CAD on protective properties of plasticized AASC concrete, mixed with seawater, to steel reinforcement was investigated.

Mass loss of steel rebars weren't fixed. This is evidence of no effect of Cl^- and SO_4^{2-} ions on steel reinforcement in plasticized AASC fine concretes, modifided by CAD and mixed with seawater.

The state of steel rebars before embedding (Fig. 9, 10) and embedded in specimens after 90 d of hardening (Fig. 11, 12) were compared.

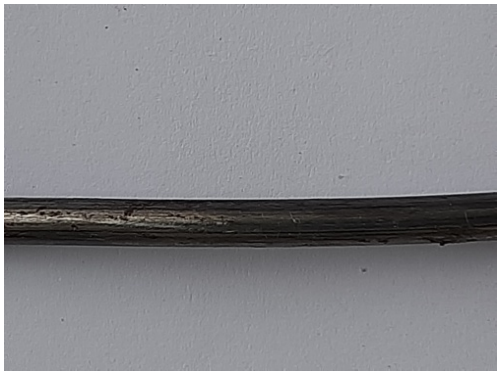

Fig. 9. Steel rebars before embedding in plasticized alkali-activated slag cement fine concrete (zoom x4) based on soda ash.

The absence of corrosion processes on surface of steel reinforcement in plasticized AASC concrete, mixed with seawater, was also confirmed by visual control.

Thus, effectiveness of CAD in plasticized AASC fine concrete for enhanced protective properties to steel reinforcement was confirmed.

Conclusion

1. Increasing of fresh concrete consistency as well as advanced strength of concrete based on alkali-activated slag cement while mixing with seawater was shown.
2. Prevention of steel reinforcement corrosion under the action of chlorides and sulfates in plasticized alkali-activated slag cement concrete mixed with seawater was ensured due to application of complex additive «portland cement - calcium aluminate cement - clinoptilolite».
3. Enhancement of protective properties of plasticized alkali-activated slag cement concrete, mixed with seawater, to steel reinforcement is explained by binding of ions Cl^- and SO_4^{2-} in Kuzel's salt (AFm phase) as well as by exchange of OH^- ions with these aggressive ions in structure of clinoptilolite.

Fig. 10. Steel rebars before embedding in plasticized alkali-activated slag cement fine concrete (zoom x4) based on sodium metasilicate.

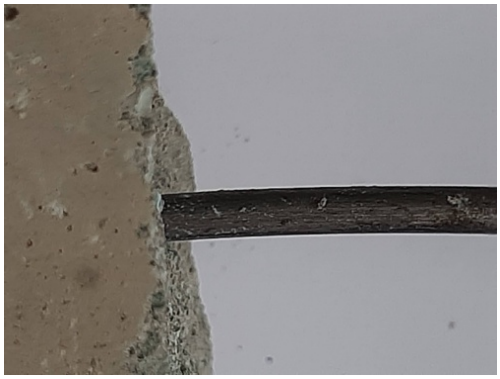

Fig. 11. Steel rebars embedded in plasticized AASC fine concrete mixed with seawater after 90 d of hardening (zoom x4) and based on soda ash.

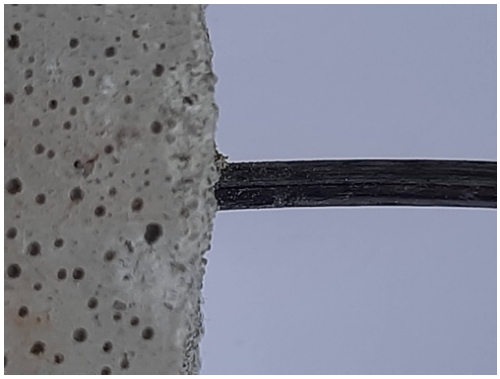

Fig. 12. Steel rebars embedded in plasticized AASC fine concrete mixed with seawater after 90 d of hardening (zoom x4) and based on sodium metasilicate.

Authors would like to acknowledge the contribution of the COST Action CA15202 «Self-Healing concrete: the path to sustainable construction» of the European Union's framework program HORIZON2020, http://www.cost.eu/COST_Actions/ca/CA15202. The authors also express their gratitude to the Ministry of Education and Science of Ukraine for financial support of this research that is carried out within the budgetary financing of topic with registration No 1020U001010 and implementation period 2020 - 2022.

References

1. V.A Abyzov, K.K. Pushkarova, M. O. Kochevykh, O.A. Honchar, N.L. Bazeliuk, Innovative building materials in creation an architectural environment. IOP Conf. Series: Materials Science and Engineering **907**, 012035 (2020). doi: 10.1088/1757-899X/907/1/012035

2. D. Anopko, O. Honchar, M. Kochevykh, L. Kushnierova, Radiation protective properties of fine-grained concretes and their radiation resistance. IOP Conf. Series: Materials Science and Engineering **907**, 012031 (2020). doi: 10.1088/1757-899X/907/1/012031

3. M. Hohol, M. Sanytsky, T. Kropyvnytska, A. Barylyak, Y. Bobitski, The effect of sulfur-and carbon-codoped TiO_2 nanocomposite on the photocatalytic and mechanical properties of cement mortars. Eastern-European Journal of Enterprise Technologies **4(6-106)**, 6–14 (2020). doi: 10.15587/1729-4061.2020.210218

4. M. Sanytsky, T. Kropyvnytska, S. Fic, H. Ivashchyshyn, Sustainable low-carbon binders and concretes. E3S Web Conf. **166**, 06007 (2020). doi: 10.1051/e3sconf/202016606007

5. T. Kropyvnytska, T. Rucinska, H. Ivashchyshyn, R. Kotiv, Development of Eco-Efficient Composite Cements with High Early Strength. Lecture Notes in Civil Engineering **47,** 211–218 (2020). doi: 10.1007/978-3-030-27011-7_27

6. T. Markiv, K. Sobol, N. Petrovska, O. Hunyak, The Effect of Porous Pozzolanic Polydisperse Mineral Components on Properties of Concrete. Lecture. Notes in Civil Engineering **47**, 275–282 (2020). doi: 10.1007/978-3-030-27011-7_35

7. T. Markiv, Kh. Sobol, M. Franus, W. Franus, Mechanical and durability properties of concretes incorporating natural zeolite. Archives of Civil and Mechanical Engineering **16,** 554–562 (2016). doi: 10.1016/j.acme.2016.03.013

8. S. Chepurna, O. Borziak, S. Zubenko, Concretes, modified by the addition of high-diffused chalk, for small architectural forms. Materials Science Forum **968**, 82–88 (2019). doi: 10.4028/www.scientific.net/MSF.968.82

9. O. Moskalenko, R. Runova, Ice Formation as an Indicator of Frost-Resistance on the Concrete Containing Slag Cement in Conditions of Freezing and Thawing. Materials Science Forum **865**, 145–150 (2016). doi: 10.4028/www.scientific.net/MSF.865.145

10. O. Bondarenko, S. Guzii, K. Zaharchenko, E. Novoselenko, Development of protective materials based on glass- and slag-containing portland cement structures. Eastern-European Journal of Enterprise Technologies **6/11(78)**, 41–47 (2015). doi: 10.15587/1729-4061.2015.56577.

11. O.Yu. Berdnyk, O.V. Lastivka, A.A. Maystrenko N.O. Amelina, Processes of structure formation and neoformation of basalt fiber in an alkaline environment. IOP Conf. Series: Materials Science and Engineering **907**. 012036 (2020). doi: 10.1088/1757-899X/907/1/012036

12. V.I. Gots, O.V. Lastivka, O.Yu. Berdnyk, O.O. Tomin, P.S. Shilyuk, Corrosion resistance of polyester powder coatings using fillers of various chemical nature. Key Engineering Materials **864**. 115–121 (2020). doi: 10.4028/www.scientific.net/KEM.864.115

13. J.L. Provis, Geopolymers and other alkali activated materials: why, how, and what? Mater Struct. **47**, 11–25 (2014). doi: 10.1617/s11527-013-0211-5

14. V.V. Chistyakov, I.G. Grankovskii, V.I. Gots, Structure formation upon hardening of slag-alkali binder. Journal of applied chemistry of the USSR. **59** (3), 542–546 (1986)

15. A. Fernández-Jiménez, J.Y. Pastor, A. Martín, A. Palomo, High-Temperature Resistance in Alkali-Activated Cement. Journal of the American Ceramic Society **93 (10)**, 3411–3417 (2010). doi: 10.1111/j.1551-2916.2010.03887.x

16. V.I. Gots, O.Y. Berdnyk, N.O. Rogozina, A.A. Maystrenko. Production of modified basalt fibre for heat-insulating products manufacturing. IOP Conference Series: Materials Science and Engineering (MSE) **708**. 012082 (2019). doi: 10.1088/1757-899X/708/1/012082

17. O. Kovalchuk, V. Grabovchuk, Ya. Govdun, Alkali activated cements mix design for concretes application in high corrosive conditions. MATEC Web of conferences **230**, 03007 (2018). doi: 10.1051/matecconf/201823003007

18. M. Cyr, R. Pouhet, The frost resistance of alkali-activated cement-based binders. Handbook of Alkali-Activated Cements, Mortars and Concretes 293–318 (2015). doi: 10.1533/9781782422884.3.293

19. Y. Savchuk, A. Plugin, V. Lyuty, O. Pluhin, O. Borziak, Study of influence of the alkaline component on the physico-mechanical properties of the low clinker and clinkerless waterproof compositions. MATEC Web of Conferences **230**,

03018 (2018). doi: 10.1051/matecconf/201823003018

20. Y.V. Tsapko, A.Yu. Tsapko, O.P. Bondarenko, M.V. Sukhanevych, M.V. Kobryn, Research of the process of spread of fire on beams of wood of fire-protected intumescent coatings. IOP Conference Series: Materials Science and Engineering **708**, 01211 (2019). doi: 10.1088/1757-899x/708/1/012112
21. Y. Tsapko, D. Zavialov, O. Bondarenko, N. Marchenco, S. Mazurchuk, O. Horbachova, Determination of thermal and physical characteristics of dead pine wood thermal insulation products. Eastern-European Journal of Enterprise Technologies **4 (10 (100))**, 37–43 (2019). doi: 10.15587/1729-4061.2019.175346
22. V. Gots, A.Gelevera, O. Petropavlovsky, N. Rogozina, V. Smeshko, Influence of whitening additives on the properties of decorative slag-alkaline cements. IOP Conf. Series: Materials Science and Engineering **907**, 012033 (2020). doi: 10.1088/1757-899X/907/1/012033
23. C. Shi, A. Fernández-Jiménez, A. Fernández-Jiménez, Stabilization/Solidification of Hazardous and Radioactive Wastes with Alkali-Activated Cements. Journal of Hazardous Materials **137(3)** 1656-63 (2006). doi: 10.1016/j.jhazmat.2006.05.008
24. G. Kochetov, T. Prikhna, O. Kovalchuk, D. Samchenko, Research of the treatment of depleted nickel-plating electrolytes by the ferritization method. Eastern-European Journal of Enterprise Technologies **3(6-93)**, 52–60 (2018). doi: 10.15587/1729-4061.2018.133797
25. A. Miller, A. Horvath, P.J.M. Monteiro, Impacts of booming concrete production on water resources worldwide. Nat. Sustain. **1**, 69–76 (2018). doi: 10.1038/s41893-017-0009-5
26. A.M. Rashad, Y. Bai, P.A.M. Basheer, N.B. Milestone, N.C. Collier, Hydration and properties of sodium sulfate activated slag. Cem. Concr. Compos. **37**, 20–29 (2013). doi: 10.1016/j.cemconcomp.2012.12.010
27. A.R. Brough, M. Holloway, J. Sykes, A. Atkinson, Sodium silicate-based alkaliactivated slag mortars: Part II. The retarding effect of additions of sodium chloride or malic acid. Cem. Concr. Res. **30**, 1375–1379 (2000). doi: 10.1016/S0008-8846(00)00356-2
28. W.K.W. Lee, J.S.J. van Deventer, The effects of inorganic salt contamination on the strength and durability of geopolymers. Colloids and Surfaces A: Physicochemical and Engineering Aspects **211** 115–126 (2002). doi: 10.1016/S0927-7757(02)00239-X
29. P.V. Krivenko, Why Alkaline Activation – 60 Years of the Theory and Practice of Alkali-Activated Materials. Journal of Ceramic Science and Technology **8**. 323–334 (2017). doi: 10.4416/JCST2017-00042
30. P. Krivenko, I. Rudenko, O. Konstantynovskyi, Design of slag cement, activated by Na(K) salts of strong acids, for concrete reinforced with steel fittings. Eastern-European Journal of Enterprise Technologies **6 (6-108)**, 26-40 (2020). doi: 10.15587/1729-4061.2020.217002
31. A.M. Rashad, M. Ezzat, A Preliminary study on the use of magnetic, Zamzam, and sea water as mixing water for alkali-activated slag pastes. Construction and Building Materials **207**, 672–678 (2019). doi: 10.1016/j.conbuildmat.2019.02.162
32. Y. Jun, T. Kim, J. H. Kim, Chloride-bearing characteristics of alkali-activated slag mixed with seawater: Effect of different salinity levels. Cement and Concrete Composites **112**, 103680 (2020). doi: 10.1016/j.cemconcomp.2020.103680
33. P. Krivenko, V. Gots, O. Petropavlovskyi, I. Rudenko, O. Konstantynovskyi, A. Kovalchuk, Development of solutions concerning regulation of proper deformations in alkali-activated cements. Eastern-European journal of Enterprise Technologies **5 (6-101)**, 24–32 (2019). doi: 10.15587/1729-4061.2019.181150
34. P. Krivenko, O. Petropavlovskyi, I. Rudenko, O. Konstantynovskyi, A. Kovalchuk, Complex multifunctional additive for anchoring grout based on alkali-activated portland cement. IOP Conference Series **907**, 012055 (2020) doi: 10.1088/1757-899X/907/1/012055
35. M. Criado, The corrosion behaviour of reinforced steel embedded in alkali-activated mortar. Handbook of Alkali-Activated Cements. Mortars and Concretes **2015**, 333–372 (2015). doi: 10.1533/9781782422884.3.333
36. S. Mundra, S. A. Bernal, M. Criado, et al., Steel corrosion in reinforced alkali-activated materials. RILEM Tech. Lett. **2**. 33–39 (2017). doi: 10.21809/rilemtechlett.2017.39
37. M.S.H. Khan, O. Kayali, Chloride binding ability and the onset corrosion threat on alkali-activated GGBFS and binary blend pastes. Eur. J. Environ. Civ. En. **22 (8)**. 1023–1039 (2018). doi: 10.1080/19648189.2016.1230522
38. H.A. Yousif, F.F. Al-Hadeethi, B. Al-Nabilsy, A.N. Abdelhadi, Corrosion of Steel in High-Strength Self-Compacting Concrete Exposed to Saline Environment. Corrosion of Steel in High-Strength Self-Compacting Concrete Exposed to Saline Environment. International Journal of Corrosion **2014**, 564163 (2014). doi: 10.1155/2014/564163
39. P. Krivenko, O. Petropavlovskyi, O. Kovalchuk, I. Rudenko, O. Konstantynovskyi, Enhancement of alkali-activated slag cement concretes crack

resistance for mitigation of steel reinforcement corrosion. E3S Web of Conferences **166**, 06001 (2020). doi: 10.1051/e3sconf/202016606001

40 Y. Jun, Y. H. Bae, T. Y. Shin, J. H. Kim, H. J. Yim, Alkali-Activated Slag Paste with Different Mixing Water: A Comparison Study of Early-Age Paste Using Electrical Resistivity. *Materials* **13**. 2447 (2020). doi: 10.3390/ma13112447

41. X. Ke, S. A. Bernal, J. L. Provis, Uptake of chloride and carbonate by Mg-Al and Ca-Al layered double hydroxides in simulated pore solutions of alkali-activated slag cement. Cem. Concr. Res. **100**. 1–13 (2017). doi: 10.1016/j.cemconres.2017.05.015

42. L. Raki, J. J. Beaudoin, L. Mitchell. Layered double hydroxidelike materials: Nanocomposites for use in concrete. Cem. Concr. Res. **34 (9)**. 1717–1724 (2004). doi:/10.1016/j.cemconres.2004.05.012

43. Q. Wang, D. O'Hare. Recent advances in the synthesis and application of layered double hydroxide (LDH) nanosheets. Chem. Rev. **112 (7)**. 4124–4155 (2012). doi: 10.1021/cr200434v.

44. X. Ke, S. A. Bernal, J. L. Provis. Chloride binding capacity of synthetic C-(A)-S-H type gels in alkali-activated slag simulated pore solutions. 1st International Conference on Construction Materials for Sustainable Future. 1–7 (2017).

45. Q. Yuan, C. Shi, G. De Schutter, K. Audenaert, D. Deng, Chloride Binding of Cement-Based Materials Subjected to External Chloride Environment – A Review. Constr. Build. Mater. **23** (1), 1–13 (2009). doi: 10.1016/j.conbuildmat.2008.02.004

46. B.A. Clark, P.W. Brown, The formation of calcium sulfoaluminate hydrate compounds, Part II. Cement and Concrete Research **30**, 233–240 (2000) doi: 10.1016/S0008-8846(99)00234-3

47. E. Pushkarova, V. Gots, O. Gonchar, Stability of hydrosulfoaluminosiljcate compounds and durability of an artificial stone based on them. Brittle Matrix Composites **8**, 399–408 (2006)

48. E. Pushkarova, V. Gots, O. Gonchar, Stability of hydrosulfoaluminosiljcate compounds and durability of an artificial stone based on them (Book Chapter). Brittle Matrix Composites **8**, 399–408 (2007), doi: 10.1533/9780857093080.399

49. L.G. Baquerizo, T. Matschei, K.L. Scrivener, M. Saeidpour, L. Wadsö, Hydration states of AFm cement phases. Cement and Concrete Research **73**, 143–157 (2015). doi: 10.1016/j.cemconres.2015.02.011

50. A.A. Plugin, O.S. Borziak, O.A. Pluhin, T.A. Kostuk, D.A. Plugin, Hydration products that provide water-repellency for portland cement-based waterproofing compositions and their identification by physical and chemical methods. Lecture Notes in Civil Engineering **100**, 328–335 (2020). 10.1007/978-3-030-57340-9_40

51. Yu.L. Nosovskyi, PhD (Eng) thesis, Kyiv, 2004

52. S.A. Bernal, Advances in near-neutral salts activation of blast furnace slags. RILEM Technical Letters **1**, 39–44 (2016). doi: 10.21809/rilemtechlett.v1.8

53. Yu.A. Sidorenko, PhD (Eng) thesis, Kyiv, 1991

54. V.I. Pushkar, PhD (Eng) thesis, Kyiv, 2010

55. C. Belviso, N. Perchiazzi, F. Cavalcante, Zeolite from Fly Ash: An Investigation on Metastable Behavior of the Newly Formed Minerals in a Medium-High-Temperature Range. Ind. Eng. Chem. Res. **58** (44), 20472–20480 (2019). doi: 10.1021/acs.iecr.9b03784

56. A. Mesbah, M.François, C. Caudit-Coumes et al. Crystal structure of Kuzel's salt $3CaO{\cdot}Al_2O_3{\cdot}1/2CaSO_4{\cdot}1/2CaCl_2{\cdot}11H_2O$ determined by synchrotron powder diffraction. Cement and Concrete Research **41**, 504–509 (2011). doi: 10.1016/j.cemconres.2011.01.015